

# Effects of gain and bandwidth on the multimode behavior of optoelectronic microwave oscillators

Y. Kouomou Chembo<sup>1,2</sup>, Laurent Larger<sup>1</sup>, Ryad Bendoula<sup>1</sup>,  
and Pere Colet<sup>2</sup>

<sup>1</sup>*Département d'Optique, Institut FEMTO-ST, 16 Route de Gray, 25030 Besançon cedex, France.*

<sup>2</sup>*Instituto de Física Interdisciplinar y Sistemas Complejos IFISC (CSIC-UIB), E-07122 Palma de Mallorca, Spain.*

[yanne.chembo@femto-st.fr](mailto:yanne.chembo@femto-st.fr)

**Abstract:** We show that when subjected to high gain, delay-line optoelectronic oscillators can display a strongly multimode behavior depending on the feedback bandwidth. We found that this dynamical regime may arise when the bandwidth of the feedback loop spans over several hundreds of ring cavity-modes, and also when the oscillator is switched on abruptly. Such a persistent multimode regime is detrimental to the performances of this system which is normally intended to provide ultra-pure and single-mode microwaves. We experimentally evidence this multimode dynamics and we propose a theory to explain this undesirable feature.

© 2008 Optical Society of America

**OCIS codes:** (130.0250) Optoelectronics; (190.3100) Instabilities and chaos; (350.4010) Microwaves.

---

## References and links

1. X. S. Yao and L. Maleki, "Optoelectronic microwave oscillator," *J. Opt. Soc. Am. B* **13**, 1725–1735 (1996).
2. L. M. Narducci, *et al.*, "Mode-mode competition and unstable behavior in a homogeneously broadened ring laser," *Phys. Rev. A* **33**, 1842–1854 (1986).
3. K. A. Winick, "Longitudinal mode competition in chirped grating distributed feedback lasers," *IEEE J. Quantum Electron.* **35**, 1402–1411 (1999).
4. A. M. Yacomotti, *et al.*, "Dynamics of multimode semiconductor lasers," *Phys. Rev. A* **69**, 053816–1-9 (2004).
5. J. L. Font, R. Vilaseca, F. Prati, and E. Roldán, "Coexistence of single-mode and multi-longitudinal mode emission in the ring laser model," *Opt. Commun.* **261**, 336–341 (2006).
6. T. Voigt, *et al.*, "Experimental investigation of RiskenNummedalGrahamHaken laser instability in fiber ring lasers," *Appl. Phys. B* **79**, 175–183 (2004).
7. C. Y. Wang, *et al.*, "Coherent instabilities in a semiconductor laser with fast gain recovery," *Phys. Rev. A* **75**, 031802(R)–1-4 (2007).
8. Y. Kouomou Chembo, L. Larger, H. Tavernier, R. Bendoula, E. Rubiola and P. Colet, "Dynamic instabilities of microwaves generated with optoelectronic oscillators," *Opt. Lett.* **32**, 2571–2573 (2007).
9. Y. Kouomou Chembo, L. Larger, and P. Colet, "Nonlinear dynamics and spectral stability of optoelectronic microwave oscillators," *IEEE J. Quantum Electron.* (in press).

---

## 1. Introduction

Narrow-bandwidth optoelectronic oscillators (OEOs) can generate ultra-pure microwave frequencies for aerospace and telecommunication applications [1]. Single-mode OEOs are able to produce very sharp-peaked radio-frequencies, with extremely low phase noise, so that they are

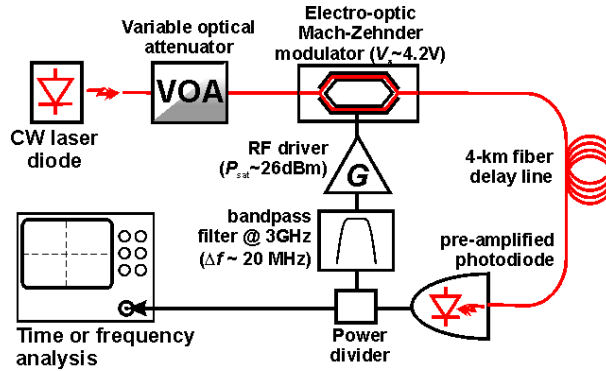


Fig. 1. Experimental setup for the single-loop OEO.

expected to be extremely useful in various areas of physics and technology where particularly high spectral purity is required. However, under certain conditions, we have observed that the OEO's behavior is highly multimode, something incompatible with its intrinsic purpose which is to provide ultra-pure microwave frequencies through single-mode operation. In fact, if multi-longitudinal mode dynamics has been thoroughly studied in other oscillators like lasers (see for example refs. [2, 3, 4, 5, 6, 7]), no study has focused on the case of OEOs. The aim of this article is therefore to evidence this multimode behavior in OEOs, and to give a theoretical insight into the mode coupling mechanisms, through time-domain modeling.

## 2. The experimental system

The system under study is a single-loop OEO [1], corresponding to the experimental set-up presented in Fig. 1. In the optoelectronic feedback loop, a continuous-wave semiconductor laser of optical power  $P$  feeds a LiNbO<sub>3</sub> Mach-Zehnder (MZ) modulator of DC and RF half-wave voltages  $V_{\pi DC} \simeq V_{\pi RF} = 4.2$  V. This MZ modulator is biased with a voltage  $V_B$ , and subjected to a radio-frequency modulation voltage  $V(t)$ . The modulated optical signal then travels through a 4-km long thermalized fiber delay-line, inducing a time-delay  $T = 20$   $\mu$ s which corresponds to a free spectral range  $\Omega_T/2\pi = 1/T = 50$  kHz. A fast amplified photodiode with a conversion factor  $S$  converts the optical signal into an electrical one, which is amplified by a microwave amplifier (RF driver) with gain  $G$ . In the electrical path, a narrow-band microwave filter is inserted in order to select the frequency range for the amplified modes; its central frequency is  $\Omega_0/2\pi = 3$  GHz, and the  $-3$  dB bandwidth is  $\Delta\Omega/2\pi = 20$  MHz (corresponding to a quality factor  $Q = \Omega_0/\Delta\Omega = 150$ ). Therefore, there are  $\Delta\Omega/\Omega_T = 400$  ring-cavity modes inside the bandwidth, and of course several thousands outside. All optical and electrical losses are gathered in a single attenuation factor  $\kappa$ .

Experimentally, when the system is switched on by continuous tuning of the OEO loop gain from below to above threshold, it oscillates in a single-mode fashion, and with an ultra-low phase noise as expected. But when the switching is abrupt above threshold, the OEO remains highly multimode even after waiting for very long transients, as it can be seen in Fig. 2. The multimode dynamics is sustained in a 4 MHz span around the central frequency of the RF filter, and the power difference between the oscillating modes and the damped modes within the filter bandwidth is approximately equal to 40 dB. This result clearly demonstrates that depending on the number of cavity modes within the RF filter bandwidth, OEOs may display a complex multimode dynamics, depending on the switching-on procedure.

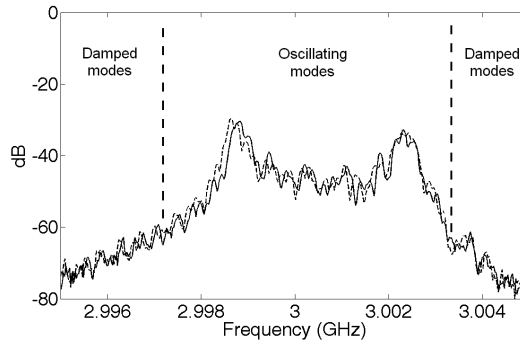


Fig. 2. Experimental radio-frequency spectrum of the OEO after 30 seconds (dashed line) and after 2 hours (continuous line), in a 10 MHz window. The modal competition can be considered in this case as permanent.

### 3. Multiple timescale analysis of the multimode behavior

Single-mode behavior in OEOs should in fact be highly counter-intuitive, because as emphasized earlier, the delay line plays the role of a cavity and thereby gives birth to thousands of longitudinal cavity-modes, amongst which hundreds are within the RF filter bandwidth. Nothing theoretically prevents all these modes to oscillate simultaneously. These modes are attached to the longitudinal resonance condition of the resonator: they are coupled through the common reservoir of energy provided by the gain, and through the MZ modulator. A single-mode operation can be obtained experimentally with a slow switch-on procedure because in this case, the modal competition just above threshold is significantly faster than the increase rate of the gain (owing to the fact that there is only a very small quantity of gain energy to compete for). On the other hand, when the OEO is abruptly switched on, all the modes are simultaneously amplified before the transient mode competition can select a single oscillating mode, and the so-called *maximum gain mode* does not systematically win the modal competition.

Our aim is to investigate the theoretical origin for this persistent multimode behavior in OEOs with the time-domain model introduced in ref. [8]. The dynamics of the dimensionless microwave variable  $x(t) = \pi V(t)/2V_{\pi_{RF}}$  is ruled by [9]

$$x + \frac{1}{\Delta\Omega} \frac{dx}{dt} + \frac{\Omega_0^2}{\Delta\Omega} \int_{t_0}^t x(s) ds = \beta \cos^2[x(t-T) + \phi], \quad (1)$$

where  $\beta = \pi \kappa SGP/2V_{\pi_{RF}}$  is the normalized feedback gain and  $\phi = \pi V_B/2V_{\pi_{DC}}$  is the Mach-Zehnder offset phase. Then, around the carrier frequency  $\Omega_0$ , the complex slowly-varying envelope  $\mathcal{A}(t) = |\mathcal{A}(t)|e^{i\psi(t)}$  of the quasi-sinusoidal microwave variable  $x(t)$  obeys

$$\dot{\mathcal{A}} = -\mu \mathcal{A} + 2\mu \gamma \text{Jc}_1[2|\mathcal{A}_T|] \mathcal{A}_T, \quad (2)$$

where  $\mu = \Delta\Omega/2$  is the half-bandwidth of the RF filter,  $\gamma = \beta \sin 2\phi$  is the effective gain of the feedback loop, and  $\text{Jc}_1$  is the *Bessel-cardinal* function defined as  $\text{Jc}_1(x) = \text{J}_1(x)/x$  [8]. We have also adopted the conventional notation  $\mathcal{A}_T \equiv \mathcal{A}(t-T)$ , and the phase matching condition  $e^{-i\Omega_0 T} = -1$  has been considered.

We have simulated the deterministic Eq. (2) with two different initial conditions, corresponding to a smooth and abrupt start for the OEO: the smooth case corresponds to the bifurcation diagrams as in [8], where the below to above threshold condition is crossed with a continuous increase of the single-mode amplitude; the abrupt start corresponds to a situation where

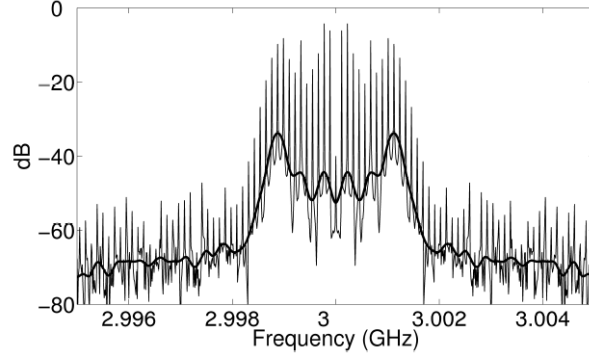


Fig. 3. Numerical simulation of the radio-frequency spectrum of the OEO after 1 s, in a 10 MHz window. The thin line represents the result of the simulation, while the thick line represents an averaging of the spectrum with a 125 kHz resolution, in order to facilitate comparison with the oscilloscope display of Fig. 2.

Gaussian random numbers are considered as initial condition in the interval  $[-T, 0]$ . The result for this latter case is displayed in Fig. 3, and it can be seen that after one second, the dynamics of the OEO is highly multimode. The oscillating modes are within a 3 MHz bandwidth and 40 dB above the damped modes, in excellent agreement with the experimental result. It should be emphasized that 1 second is a macroscopic timescale for this system, for which the largest time-scale is  $T = 20 \mu\text{s}$ . Hence, this simulation confirms that a persistent multimode behavior is observed, which may or not lead to a single-mode behavior after a transient process which is very long.

To provide an analytical insight into the multimode behavior of the OEO, we use a multiple time scale analysis to decompose the dynamics according to the three timescales  $\Omega_0$ ,  $\mu$  and  $\Omega_T$  which are separated by the same three orders of magnitude. Considering the smallness (or separation) parameter  $\varepsilon \sim 10^{-3}$ , the initial microwave variable oscillations can be expanded as

$$x(t) = \sum_{k=0}^3 \varepsilon^k x_k(T_0, T_1, T_2, T_3) + \mathcal{O}(\varepsilon^4), \quad (3)$$

while its amplitude expands as

$$|\mathcal{A}(t)| = \sum_{k=0}^3 \varepsilon^k |\mathcal{A}|_k(T_0, T_1, T_2, T_3) + \mathcal{O}(\varepsilon^4), \quad (4)$$

where  $x_k$  and  $|\mathcal{A}|_k$  are associated to the timescales  $T_k = \varepsilon^k t$ . The time derivative can also be expanded as  $d/dt = \sum_{k=0}^3 \varepsilon^k D_k$  where  $D_k = \partial/\partial T_k$ . If we rescale the temporal parameters as  $\mu = \varepsilon \hat{\mu}$  and  $\Omega_T = \varepsilon^2 \hat{\Omega}_T$ , the timescale components of the integral variable  $u(t) = \int_{t_0}^t x(s) ds$  obey the following equations at the various orders of  $\varepsilon$ :

- Order  $\varepsilon^0$

$$D_0^2 u_0 + \Omega_0^2 u_0 = 0 \quad (5)$$

- Order  $\varepsilon^1$

$$\begin{aligned} D_0^2 u_1 + \Omega_0^2 u_1 &= -2D_0 D_1 u_0 - 2\hat{\mu} D_0 u_0 \\ &\quad + 2\hat{\mu} \gamma J_1 [2|\mathcal{A}_{0T}|] \times \cos[\Omega_0 T_0 + \psi_T] \end{aligned} \quad (6)$$

- Order  $\varepsilon^2$

$$D_0^2 u_2 + \Omega_0^2 u_2 = -2D_0 D_1 u_1 - (D_1^2 + 2D_0 D_2) u_0 - 2\hat{\mu}(D_0 u_1 + D_1 u_0) + 2\hat{\mu}\gamma \left\{ 2|\mathcal{A}_{1T}| J_1' [2|\mathcal{A}_{0T}|] \right\} \times \cos[\Omega_0 T_0 + \psi_T] \quad (7)$$

- Order  $\varepsilon^3$

$$D_0^2 u_3 + \Omega_0^2 u_3 = -2D_0 D_1 u_2 - (D_1^2 + 2D_0 D_2) u_1 - 2(D_0 D_3 + D_1 D_2) u_0 - 2\hat{\mu}(D_0 u_2 + D_1 u_1 + D_2 u_0) + 2\hat{\mu}\gamma \left\{ 2|\mathcal{A}_{2T}| J_1' [2|\mathcal{A}_{0T}|] + 2|\mathcal{A}_{1T}|^2 J_1'' [2|\mathcal{A}_{0T}|] \right\} \times \cos[\Omega_0 T_0 + \psi_T] \quad (8)$$

These equations correspond to the various dynamical behaviors at each timescale. From Eq. (5) corresponding to order  $\varepsilon^0$ , we can deduce that  $u_0$  is sinusoidal, so that its integrand  $x_0$  may also be expressed as

$$x_0 = \frac{1}{2} \mathcal{A}(T_1, T_2, T_3) e^{i\Omega_0 T_0} + \frac{1}{2} \mathcal{A}^*(T_1, T_2, T_3) e^{-i\Omega_0 T_0}, \quad (9)$$

which corresponds to our initial hypothesis of quasi-sinusoidal oscillations for  $x$ . The spectral splitting of  $\Omega_0$ ,  $\mu$  and  $\Omega_T$  suggests the following decomposition

$$\mathcal{A}(T_1, T_2, T_3) = A(T_1) \sum_{n=-N}^N a_n(T_3) e^{in\hat{\Omega}_T T_2}, \quad (10)$$

where  $2N = \mu/\Omega_T$  is the number of cavity modes inside the bandwidth. The dynamics of the system is therefore ruled by the slow complex amplitude  $A(T_1)$  associated to the carrier  $\Omega_0$ , and the even slower complex modal amplitudes  $a_n(T_3)$  associated to the detuning frequencies  $n\Omega_T$ . This modal decomposition enables the expansion of the amplitude according to

$$\begin{aligned} |\mathcal{A}|_0 &= \Omega_0 |A| \left| \sum_{-N}^N a_n e^{in\hat{\Omega}_T T_2} \right| \\ |\mathcal{A}|_1 &= \frac{1}{2|A|} i \left( \frac{\partial A^*}{\partial T_1} A - A^* \frac{\partial A}{\partial T_1} \right) \left| \sum_{-N}^N a_n e^{in\hat{\Omega}_T T_2} \right| \\ |\mathcal{A}|_2 &= \frac{1}{2\Omega_0 |A|} \left| \frac{\partial A}{\partial T_1} \right|^2 \left| \sum_{-N}^N a_n e^{in\hat{\Omega}_T T_2} \right| + \frac{1}{2} \hat{\Omega}_T |A| \\ &\quad \times \frac{\left[ \sum_{-N}^N a_n e^{in\hat{\Omega}_T T_2} \sum_{-N}^N n a_n^* e^{-in\hat{\Omega}_T T_2} + \text{c.c.} \right]}{\left| \sum_{-N}^N a_n e^{in\hat{\Omega}_T T_2} \right|}, \end{aligned} \quad (11)$$

where “c. c.” stands for the complex conjugate of the preceding term.

The dynamical equation ruling the dynamics of the slow variation  $A(T_1)$  of the carrier is obtained by setting to zero the secular term in Eq. (6), thereby yielding

$$\frac{\partial A}{\partial T_1} = -\hat{\mu}A + 2\hat{\mu}\gamma \frac{J_1 [2|\mathcal{A}|_{0T}]}{[2|\mathcal{A}|_{0T}]} A_T. \quad (12)$$

It is interesting to note that the amplitude  $A(T_1)$  which represents the fastest dynamics of the microwave envelope obeys an equation similar to the original Eq. (2). In fact, both equations are identical in the single-mode approximation, that is  $a_n \equiv 0$  excepted for  $n = 0$ .

On the other hand, the dynamics of the modal amplitudes  $a_n(T_3)$  are obtained after projection onto  $e^{-in\hat{\Omega}_T T_2}$  of the secular equation obtained from Eq. (8), yielding

$$\begin{aligned} \frac{\partial a_n}{\partial T_3} = & -in \frac{\hat{\Omega}_T}{\Omega_0} \left\{ \hat{\mu} + \frac{1}{A} \frac{\partial A}{\partial T_1} \right\} a_n \\ & + 2\hat{\mu}\gamma \frac{A_T}{A} a_n \times \frac{\left\{ 2|\mathcal{A}_{2T}|J_1' [2|\mathcal{A}_{0T}|] + 2|\mathcal{A}_{1T}|^2 J_1'' [2|\mathcal{A}_{0T}|] \right\}}{\left[ 2|A_T| \cdot \left| \sum_{-N}^N a_n e^{in\hat{\Omega}_T T_2} \right| \right]}, \end{aligned} \quad (13)$$

where the  $|\mathcal{A}|_n$  are defined in Eq. (11). The coupled system of Eqs. (12) and (13) constitutes the final result of the modal analysis. They may enable to understand the intrinsic mechanisms of the mode competition in OEOs.

From the multiple time scale analysis, it appears that in the multimode regime, the system is constituted by hundreds of microwave ring-cavity modes which are strongly and nonlinearly coupled through the Mach-Zehnder interferometer. It can be seen in Eq. (13) that the modal variables  $a_n$  are subjected to a nonlinear global coupling, along with winding frequency terms which are stronger as the modal frequency detunings  $n\Omega_T$  increase. It is worth noting that the modes have not been coupled phenomenologically as it is sometimes done in the literature: here, the coupling emerges naturally from the intrinsic nonlinearity of the system. This global nonlinear coupling is indeed very complex, if one remembers that terms as complicated as those of Eq. (11) are involved in the modal dynamics. This complexity is of course intrinsic to the original Eq. (2) ruling the total amplitude  $\mathcal{A}(t)$ , and which does not consider *a priori* any form of modal structure. Here as in other multimode systems, the key advantage of modal expansion is therefore to track the dynamics of individual modes, and to give an explicit insight into the topological nature of their coupling.

#### 4. Conclusion

In conclusion, we have given experimental and theoretical evidence of persistent multimode behavior in OEOs depending on the switch-on procedure. To the best of our knowledge, earlier studies on OEOs have never reported such multimode behavior. This behavior may however be interesting for several reasons. From a purely theoretical point of view, the OEO provides an excellent opportunity to investigate the dynamics of a huge quantity of globally coupled cavity-modes, at the opposite of the usual cases where only very few of them are considered. From a technological point of view, procedures like active mode-locking do address individual modes, and can not be studied properly if the system is not modeled through a modal dynamics approach. However, the study suggests that the multimode dynamics may be suppressed either with extremely selective RF filters, or either with a proper switch-on procedure. A deeper investigation on these multimode aspects is likely to open the way to many interesting applications.

#### Acknowledgment

Y. K. C. acknowledges a research grant from the *Région de Franche-Comté*, France. The authors also acknowledge financial support from the *Ministerio de Educación y Ciencia* (Spain) and from FEDER under grant TEC2006-10009 (PhoDeCC).